MECHANICAL MODEL AND MATHEMATICAL ANALYSIS FOR DUCTILE FRACTURE

Wang Tzu Chiang

Institute of Mechanics, Academia Sinica, Beijing, China

ABSTRACT

In this paper, two mechanical models are proposed to include the important influence of the micro voids, nucleated around the large second-phase particle and the models can be used to analyse the initiation of crack growth and the stable crack growth. By means of the large plastic deformation equation, the mathematical analysis was made. The finite element method and the incremental tangent stiffness method are used in numerical calculation. All the three criteria of the true fracture strain, the maximum equivalent plastic strain and the true fracture stress of the fracture process zone have been discussed. Calculations and analyses have been made to compare with some typical experimental data. Some clear mechanical pictures for the physical processes of ductile fracture are obtained.

KEYWORDS

Ductile fracture; mechanical models; initiation of crack growth; stable crack growth; fracture criteria.

INTRODUCTION

Many authors have investigated the problem of ductile fracture, The McClintock's theory of void growth, Thomason's void coalescence theory and the Rice and Johnson's theory of coalescence between crack and void are all well-known.

Krafft (1964) proposed the idea of fracture process zone, while he investigated the influence of second-phase particle on the plane strain fracture toughness K_{Ic}. Broberg (1971) elucidated further the important role of the fracture process zone.

Incorporating the idea of the fracture process zone with the two-dimension model proposed by Thomason (1968), Rice and Johnson (1970) for ductile fracture, two mechanical models are proposed in this paper, in which the important influence of micro-voids is considered. The first model is for the initiation of crack growth, while the second model is for the stable growth of crack. By means of the

large plastic deformation equations, which take into account of geometrical and physical nonlinearities, mathematical analyses with finite element method have been made. All the three criteria of the true strain, equivalent plastic strain and the true stress of fracture process zone have been discussed. Calculations and analyses have been made to compare with some typical experimental data. Some clear mechanical pictures for the physical processes of ductile fracture are obtained.

MECHANICAL MODELS

Many research works for the micromechanism of ductile fracture, have sketched out a fundamentally clear picture. In this physical picture, the nucleation of micro voids is often shown to be the first step of ductile fracture. For most of the engineering materials, the cohesion of either the medium size particles or dispersoids with the matrix is very strong. However, the cohesion is very weak for the large particle. When the matrix has undergone only some small plastic deformations, the large second-phase particles will firstly fracture to form micro voids. Then the voids will grow further with increase of plastic deformations. When the ligament of the main crack and the nearest void becomes thinner and thinner, the true stress in the ligament becomes greater and greater. Then the internal necking between the main crack and the nearest void takes place. After that, the small microscopic voids are formed around the sub micron particles. As soon as the small voids are formed. They will immediately coalesce and cause the fracture of the ligament.
Both the shape and size of the large second-phase particles are very irregular, but along the thickness direction the statistical average values can be obtained. The large second-phase particles are usually of three dimension structure. Along the thickness direction, there is the matrix material, which connects voids with each another. But three dimensional analysis is quite difficult, so instead of it, two dimensional models are established.

Mechanical Model for the Initiation of Crack Growth

As shown in Fig.1, in the vicinity of the crack tip, we take out two voids for consideration. One of is ahead of the crack tip and the other is just behind the crack tip. These two voids are assumed to have dominant influence on the initiation of crack growth.
The zone between these voids is called the fracture process zone, which contains the submicron particles.
The fracture process zone can be regarded as a micro compact tension specimen, loaded through the external zone, which can be regarded as a "loading device".
The initiation of crack growth is a process of coalescence between the main crack and void A1, that is a fracture process of the micro compact tension specimen. Like the macro uniaxial tension test, it undergoes the whole deformation process of elastic-plastic deformation, necking and final rupture, which is caused by the formation, growth and coalescence of small voids.

Mechanical Model for the Stable Crack Growth

The stable crack growth is slightly different from the initiation of crack growth. In the latter, it is a coalescent process of the main crack with the nearest void A1. But the process, following the initiation growth, is a coalescence of the void A1 with the void A2. This process can be regarded as the rupture process of a micro uniaxial tension specimen (as shown in Fig.2). So the process of stable crack growth is just a propagation process of crack from one void to another void. These processes are not continuous but carry on step by step. Each step corresponds to a rupture process of one fracture process zone, also corresponds a rupture process of a micro uniaxial tension specimen. Therefore, the analysis for stable crack growth must deal with the deformation process of a micro uniaxial tension specimen.
If all of the voids, which lie on the crack propagation face, should be considered, it will require too large a computer storage. For simplicity, a mechanical model as shown in Fig.3, is suggested.

The coalescent process of the main crack with the void A1 and the deformation process of the fracture process zone between void A1 and void A2 will be considered in detail. The coalesence of the main crack with the void A1 means that the force originally acted on the ligament between the main crack and the void A1 will be released to zero.
In fact this release process has already started, while the internal necking takes place in the zone between the main crack and the void A1. Therefore in the following analysis, the initiation point of internal necking in the zone between the main crack and the void A1 is taken as the critical point of the initiation of crack growth.

METHOD OF ANALYSIS

The fundamental equations under large plastic deformation are proposed by Hill (1959). By means of the Eulerian coordinate description and incremental theory, the fundamental equations are equivalent to the following variational formulas:

$$\delta U = \int_V \overset{(1)}{\mathbf{f}} \cdot \tilde{\mathbf{v}}\, dv - \int_{S_\sigma} \overset{(1)}{\mathbf{P}} \cdot \tilde{\mathbf{v}}\, ds \qquad (1)$$

$$U = \frac{1}{2}\int \Big\{ 2\mu \Big[d_{ij} d_{ij} - \frac{\nu}{(1-2\nu)} (d_{ii})^2 - \frac{\alpha}{g_*} (n_{ij} d_{ij})^2 \Big] - \sigma_{ij} \left(d_{ik} d_{jk} - v_{k,i} v_{k,j} \right) \Big\} dv, \qquad (2)$$

where $\mathbf{v}$ is the true velocity fields, $\tilde{\mathbf{v}}$ is the virtual velocity fields. For the fundamental equations, including the geometrical and physical nonlinearities, it is difficult to obtain an analytical solution. Usually, the finite element method is employed for numerical solution. The finite element formulas have been given by works (McMeeking, 1977; Wang, 1979).
By using the incremental tangent stiffness method, available results can be obtained. Different mesh division may affect the calculated results. So within the limit of compute storage the finest meshes should be used.

In order to reduce the errors in calculation, we assume that in the fracture process zone, same mesh is adopted, so it does not depend on the shape and size of the specimen, nor on the loading manner, but only on the shape and size of the fracture process zone and comprehensive consideration of computer storage, economy and accuracy.

To obtain the true stress and the nominal stress, acted on the section AA* as shown in Fig.2, we calculate the corresponding nodal force on the section. Dividing it by the size of the original ligament, we get the nominal stress. Dividing it by the deformed ligament, we obtain the true stress. The true strain can be calculated by:

$$\varepsilon = \ln (A_0 / A), \tag{3}$$

where A_0 is the size of the original ligament, A is the size of the deformed ligament.

COMPUTED RESULTS AND ANALYSIS

Choose two materials for typical computations. One is the high strength aluminum alloy 7075-T7351 (Van Stone, Merchant and Jr. Low 1974; Hahn and Rosenfield, 1975). The mechanical properties of this material are:

$$\sigma_{ys} = 391 \text{MPa}, \qquad K_{Ic} = 30.9 \text{MPa}\sqrt{\text{m}} \tag{4}$$

The equivalent stress-strain curve is:

$$\sigma = A \cdot \varepsilon^{n},$$

$$A = 638 \text{MPa}, \qquad n = 0.097, \tag{5}$$

The size d of the fracture process zone is approximately equal to 11.6 μm. The diameter D of the large second-particles is:

$$D = d \cdot \sqrt[3]{\frac{6}{\pi} \frac{f_v}{(1 - f_v)}} = 4.3\,\mu\text{m}. \tag{6}$$

Where f_v is the volume fraction of the large second phase particles.

The adopted macro compact tension specimen with its geometrical demensions is shown in Fig.4. The mesh division is shown in Fig.5. Using the method (Yamada, Yoskimura and Sakurai, 1968), the elements will reach plasticity one by one under incremental loading, which is restricted to within 1% or 0.5% of the limit load at each step. After the limit, we change the generalized time parameter to be the displacement at loading point, then the incremental analysis can be continued. Conventionally the whole loading process is divided into 150~250 steps.

The correlation curve between the true stress σ_y, the nominal stress σ_y^*, the true strain ε in the fracture process zone and the stress intensity factor K_I is shown in Fig.6. The correlation curve of σ_y, σ_y^* and ε is shown in Fig.7.

Choose another high strength aluminum alloy 7075-T6 for computation. The mechanical properties of this material are (Broek, 1973):

$$\sigma_{ys} = 499 \text{MPa}, \qquad \sigma_u = 553 \text{MPa}, \tag{7}$$

The equation for the stress-strain curve under the uniaxial tension is:

$$\sigma = \sigma_{ys} (\varepsilon / \alpha)^{n}, \tag{8}$$

$$n = 0.051, \qquad \alpha = 0.02,$$

The size d of the fracture process zone is approximately equal to 12 μm. The diameter D of the large second-phase particles is equal to 4.67 μm.

The calculation for the second mechanical model of the stable crack growth has been made. The correlation curve of σ_y, σ_y^*, ε for the fracture process zone between void A1 and void A2 and K1 is shown in Fig.8. It is noticeable that in every curve there is a sudden change part. This sudden change corresponds to the coalescence of the main crack with the void A1. Because of this coalescence, the forces acting on the ligament between the main crack and the void A1, will transmit to the ligament ahead of A1, resulting in a sudden change in the force at the cross section of the ligament between voids A1 and A2. But during this coalescence the external loading is kept constant, therefore K1 has only a slight change.

The correlation curve of σ_y, $\overset{*}{\sigma}_y$ and ε is shown in Fig.9. It merits attention that this curve goes smoothly without any sudden change. In fact, this curve is a correlation curve of the stress and strain for micro compact tension specimen. The sudden change in the "external load" has an important influence on the shape of this curve, but does not cause discontinuity. Another point of great interest is that the internal necking in the fracture process zone has already taken place before the coalescence of the main crack and the void A1. This is due to the fact that in the vicinity of the crack tip there is a higher triaxial tension with a smaller plastic deformation than that in the zone between voids A1 and A2. This will cause the necking to appear firstly in the zone between voids A1 and A2.

From Fig.9, it is shown that the stress-strain curves for fracture process zone are very similar to the corresponding curves of macro uniaxial tension specimen. Curve OA* indicates the elastic deformation, then A*B* is related to the plastic deformation and the plastic flow occurs after point B*. The curve C*D* indicates the coalescent process of the main crack and the void A1. After point D*, further unstable plastic flow will continue to occur until the final fracture of the ligament between the voids A1 and A2.

From Fig.8, it is shown that there is a definite relation between $\sigma_y, \delta_y, \varepsilon$ and the stress intensity factor K1. These functional relation are independent with the size and geometry of macro specimen. Therefore the true fracture stress $(\sigma_y)_f$ and the true fracture strain $(\varepsilon)_f$ can be considered as critical parameters characterizing the rupture of fracture process zone. For this material K_{IC} is equal to 20.6 $MPa\sqrt{m}$. From Fig.8, we obtain:

$$(\sigma_y)_f = 1510\,MPa, \qquad (\varepsilon)_f = 0.706, \qquad (9)$$

For small macro specimens, we can establish the relationship between $(\sigma_y)_f$, $(\varepsilon)_f$ and J_{IC}. So in the range of large scale plastic yielding, $(\sigma_y)_f$, $(\varepsilon)_f$ can be also regarded as material parameters to characterize the rupture of fracture process zone.

At present we consider the influence of the large second phase particles on K_{IC} by the second mechanical model. Works (Schwalbe, 1977; Mulherin and Rosenthal, 1971) have offered a correlation between the volume f_v of the second-phase particles and K_{IC} for high strength aluminum alloy 7075-T6. In our calculation, we put D = 4.67μm. The size of the fracture process zone can be calculated by the following formula:

$$d = D \Big/ \sqrt[3]{\frac{6}{\pi} f_v / (1 - f_v)}\,, \qquad (10)$$

The calculated results are shown in Fig.10, in which ε_{pmax} is the maximum equivalent plastic strain. Owing to the nonuniform stress fields at the crack tip, the maximum equivalent plastic strain ε_{pmax} does not take place at the centre of the micro uniaxial tension specimen but rather on the left side. As the final rupture of fracture process zone will be controlled by the nucleation of submicron particles, it is suitable to choose $(\varepsilon_{pmax})_f$ as a basic material parameter.

From Fig.10, it is shown that $(\varepsilon)_f$ has a significant variation with the volume fraction f_v, but $(\varepsilon_{pmax})_f$ remains practically constant. We consider $(\varepsilon_{pmax})_f$ as a material constant, Let:

$$(\varepsilon_{pmax})_f = 1.21,$$

From this we obtain the variation of calculated values of K_{IC} with f_v. As shown in Fig.11, the calculated results are in good agreement with the experimental data.

REFERENCES

McClintock, F.A. (1968). In Ductility, chap.9, 255, ASM.
Thomason, P. F. (1968). J. Inst. of Metals, 96, 360.
Rice, J.R. and M.A.Johnson (1970). In M.F.Kanninen (Ed.), Inelastic behavior of solids, McGraw-Hill, 614.
Krafft, J.M. (1964). Appl. Materials Research, 3, 88-101.
Broek, D. (1974). Engng. Fracture Mechanics, 6, 173-181.
Schwalbe, K.H. (1977). Engng. Fracture Mechanics, 9, 795-832.

Hill, R. (1959). J. Mech. Phys. Solids, 7, 209-225.
McMeeking, R.M. (1977). J. Mech. Phys. Solids, 25, 357-382.
Wang, T.C. (1979). Fundamental equations for the large plastic deformation and its finite element formulas, Research Paper of Institute of Mechanics, Academia Sinica.
Yamada, Y. Yoskimura N. and T. Sakurai (1968). Inter. J. Mechanic Science, 10, 343-354.
Hahn, G.T. and A.R. Rosenfield (1975). Metallurgical transaction A, 6A, 654-668.
Van Stone, R.H., R.H.Merchant and J.R.Jr. Low (1974). In Fatigue and Fracture Toughness-Cryogenic Behavior, ASTM STP 556, American Society for Testing and Materials, 93-124.

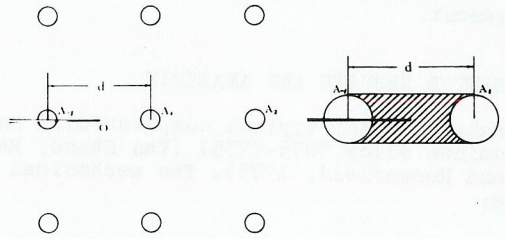

Fig. 1. Mechanical model for the initiation of crack growth.

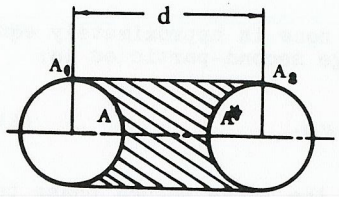

Fig. 2. Micro uniaxial tension specimen

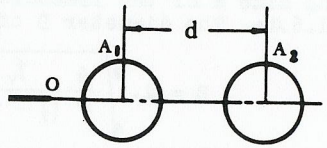

Fig. 3. Mechanical model for the stable growth of crack

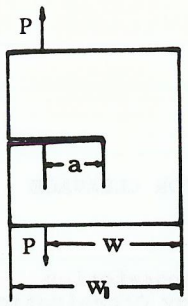

Fig. 4. Compact tension specimen

$W_1 = 3.712$ mm, $W/W_1 = 0.8$, $a/W = 0.5$,

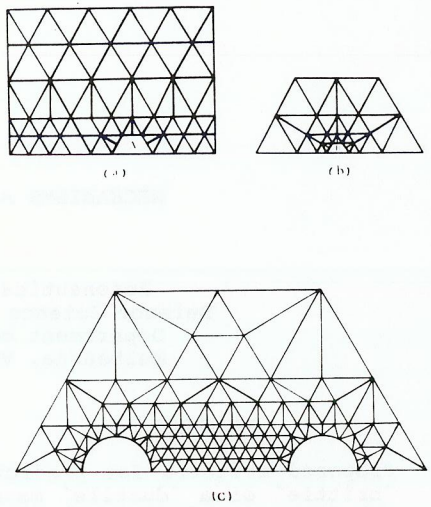

Fig. 5. Finite element mesh. (a) global mesh. (b) detail mesh in position A. (c) detail mesh in position B.

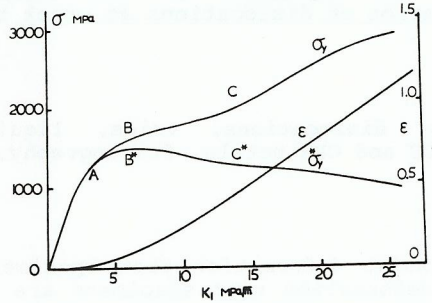

Fig. 6. Correlation curves of σ_y, σ_y^*, ε and K_1.

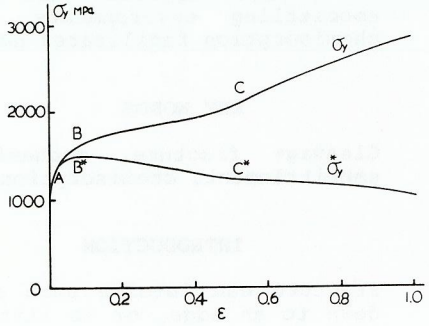

Fig. 7. Correlation curves of σ_y, σ_y^* and ε.

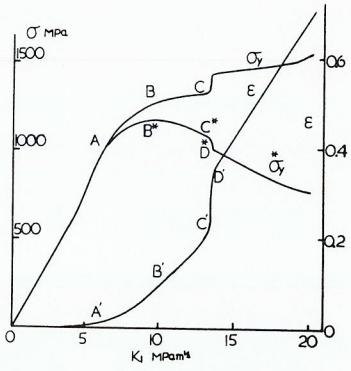

Fig. 8. Correlation curves of σ_y, σ_y^*, ε and K_1.

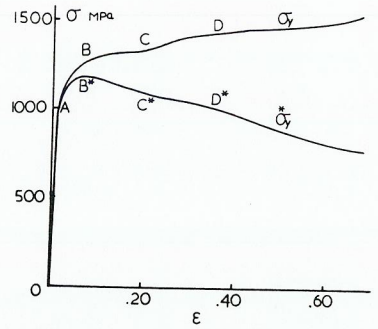

Fig. 9. Correlation curves of σ_y, σ_y^* and ε.

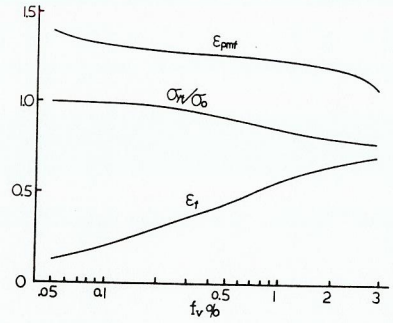

Fig. 10. $(\varepsilon)_f$, ε_{pmf}, $(\sigma_y)_f$ versus volume fraction of inclusion. $\varepsilon_{pmf} = (\varepsilon_{pmax})_f$, $\sigma_0 = 1960$ MPa.

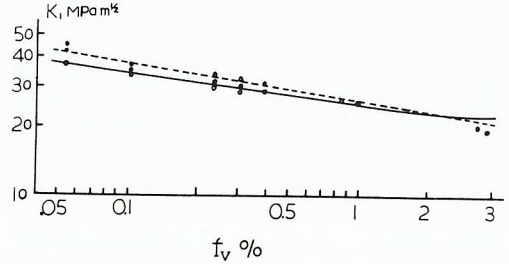

Fig. 11. Theoretical and experiment results for fracture toughness K_{Ic}. ——— calculation curve of this paper. -------- Hahn and Rosenfield formula.